

Effect of Molecular Orientational Correlations on Solvation Free Energy Computed by Reference Interaction Site Model Theory

Shoichi Tanimoto,[†] Norio Yoshida,^{*,†} Tsuyoshi Yamaguchi,[‡] Seiichiro L. Ten-no,[§] and Haruyuki Nakano[†]

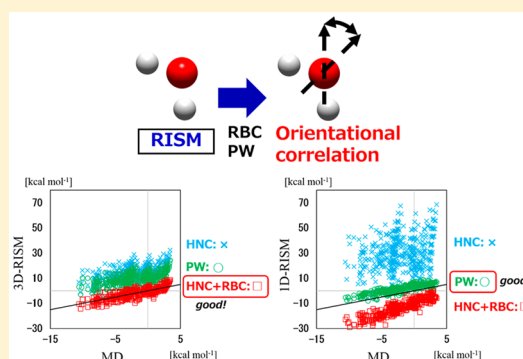
[†]Department of Chemistry, Graduate School of Science, Kyushu University, 744 Motoooka, Nishi-ku, Fukuoka 819-0395, Japan

[‡]Graduate School of Engineering, Nagoya University, Chikusa-ku, Nagoya 464-8603, Japan

[§]Graduate School of Science, Technology, and Innovation, Kobe University, Nada-ku, Kobe 657-8501, Japan

S Supporting Information

ABSTRACT: The effect of molecular orientational correlations on the solvation free energy (SFE) of one-dimensional and three-dimensional reference interaction site models (1D- and 3D-RISM) is investigated. The repulsive bridge correction (RBC) and the partial wave (PW) expansion are representative approaches for accounting for the orientational correlation partially lacking in original 1D- and 3D-RISM. The SFEs of 1D- and 3D-RISM for a set of small organic molecules are compared with the simulation results. Accordingly, the SFE expressions, based on RBC and PW, provide more accurate results than those of the uncorrected HNC or KH SFE expressions, which indicates that accounting for molecular orientational dependencies significantly contributes to the improvement of the SFE. The SFE component analysis indicates that the nonpolar component mainly contributes to the correction. The dependence of the error in the RISM SFE on the number of solute sites is examined. In addition, we discuss the differences between 1D- and 3D-RISM through the effect of these corrections.



1. INTRODUCTION

The reference interaction site model (RISM) and its three-dimensional variant (3D-RISM)^{1–5} are powerful tools for investigating the solvation thermodynamics of molecules in solution. (Hereinafter, we refer to the RISM theory as 1D-RISM to differentiate from 3D-RISM.) These methods are derived from the molecular Ornstein–Zernike integral equation theory by applying the interaction site model for the solute and solvent molecules in 1D-RISM and for the solvent molecules in 3D-RISM. These methods provide solvation structures with atomistic solute–solvent interactions to enable the calculation of solvation free energy (SFE) at a reasonable computational cost compared to those of molecular simulations. This is because both thermodynamic and configuration integrals upon solvation can be performed analytically within the RISM framework. Due to these features, 1D- and 3D-RISM have been applied to various chemical reactions in solution,^{6–11} molecular recognition,^{12–14} ion permeation,^{12,15} and aggregation.^{16,17}

To date, intensive efforts have been devoted to improving the accuracy of RISM methods. Palmer et al. found that the error in the SFE of 3D-RISM strongly correlates with the partial molar volume (PMV) of solute molecules,¹⁸ and they proposed the universal correction method using the PMV with empirical parameters. Truchon et al. showed that the clear source of errors in the SFE of 3D-RISM is the nonpolar

component of SFE that originates from the cavity formation, while the electrostatic component exhibits good correlation with molecular simulations.¹⁹ Several authors, thereafter, have proposed other corrections,^{19–24} thereby significantly improving the accuracy of SFE for small molecules including ions calculated using 1D- and 3D-RISM in aqueous solutions and nonaqueous solution.^{25–32}

In the RISM formalism, there are two sources of error in the SFE: the approximations in closure relations and the use of the interaction site model (ISM).

The hypernetted-chain (HNC)² and the Kovalenko–Hirata (KH)³³ closures have been widely used in the literature. The HNC closure for a simple liquid is derived ignoring the bridge function, which is inherently nonzero, in the exact closure equation. The site–site HNC closure is derived from the analogy of the simple liquid case. Because the site–site HNC closure is including improper diagrams, it is impossible to define the bridge function in RISM as missing diagrams in the HNC closure.³⁴ The KH closure is obtained by partially linearizing the HNC closure. The absence of bridge-type contribution leads to a significant error for the thermodynamic quantities of RISM.^{18,19,35–39} Miyata and Thapa assessed the

Received: April 20, 2019

Published: August 13, 2019

accuracy of the HNC and KH closures in terms of SFE for a simple Lennard-Jones (LJ) solution.³⁶

The use of the ISM is another major source of error in SFE. We can address the following three issues introduced for the formulation of RISM with ISM. First, the site–site total correlation functions are defined as the integration of the six-dimensional (6D) molecular pair correlation function over the orientations of molecules. Second, a superposition approximation is applied to the direct correlation function. In this approximation, the molecular direct correlation function, which is a 6D function, is approximated as a sum of spherically symmetric site–site direct correlation functions. Third, the HNC and KH closures from the theory of simple liquids are used for each of the pairs of molecular sites separately, as if the sites were free spherical particles not correlated to each other. This means that the information related to the molecular structure is not directly incorporated into the closure. These approximations have significantly deteriorated the accuracy of RISM, particularly for determining SFE.^{40–43}

Several approaches to ameliorate the lack of orientational correlation have been proposed. One is the repulsive bridge correction (RBC) by Kovalenko and Hirata.⁴⁴ They argued that RISM/HNC underestimates the three-body correlation of water sites near the hydrophobic solute, which results in the overestimation of water ordering around the solute, leading to the overestimation of the entropic component in the SFE expression. To overcome this problem, they applied RBC to the HNC closure to incorporate the solvent intramolecular correlation. Several correction methods have been proposed based on RBC.^{45,46} Another approach considering the orientational correlation is the distributed partial wave (PW) expansion by Ten-no and Iwata.^{40,41} In this approach, SFE was calculated from the PW expansion form of the molecular OZ (MOZ) equation using the correlation functions of RISM/HNC. Chuev et al. proposed a combined PW and excluded volume correction method.⁴⁷ These approaches have significantly improved the determination accuracy of SFE for several organic molecules and rare gas atoms.^{40,44,48,49}

In this study, we focus on the RBC and PW expansion methods. Although a number of systematic surveys on the properties of SFE expressions have been conducted,^{19,36–40,48–52} as far as we know, no investigation from the viewpoint of correction for molecular orientations has been reported. It is expected that a detailed analysis of these two approaches would facilitate a more sophisticated treatment of integral equation theories. Therefore, we examine the test set of small organic molecules, which is widely used for the assessment of SFE.⁵³ The SFEs evaluated by free energy perturbation (FEP) are used as a reference. In addition, the bulk solvent pressure expressions derived using the RBC and PW methods are also discussed. The aim of our study is to quantitatively compare the SFE expressions in 1D- and 3D-RISM theories and investigate how the presence of site correlation information in the SFE expressions affects the accuracy of the SFE.

2. THEORY

In this section, we briefly describe the SFE expressions within the framework of 1D- and 3D-RISM. The details of these theories can be found in the literature.^{1,2,4,5}

2.1. SFE in 1D- and 3D-RISM. The SFE can be generally evaluated using the following Kirkwood charging formula

$$\Delta\mu = \rho \int_0^1 d\lambda \int dx_1 dx_2 u(\mathbf{x}_1, \mathbf{x}_2) g(\mathbf{x}_1, \mathbf{x}_2; \lambda) \quad (1)$$

where u and g represent the intermolecular potential and distribution function, respectively; λ , the charging parameter; and \mathbf{x}_1 and \mathbf{x}_2 denote the full coordinates (position and orientation) of molecules 1 and 2, respectively.² $\lambda = 0$ and $\lambda = 1$ correspond to the unsolvated and solvated states, respectively. ρ is the number density of the pure solvent. The HNC-SFE expression, which is derived from eq 1 assuming the HNC closure, is the following

$$\Delta\mu^{\text{HNC}} = \frac{4\pi\rho}{\beta} \sum_{\alpha i} \int drr^2 \left[-c_{\alpha i}(r) - \frac{1}{2} h_{\alpha i}(r) c_{\alpha i}(r) + \frac{1}{2} \{h_{\alpha i}(r)\}^2 \right] \quad (2)$$

which is known as the Singer–Chandler expression.⁵⁴ Similarly, using the KH closure and 1D-RISM equation, the SFE for the KH approximation is derived as

$$\Delta\mu^{\text{KH}} = \frac{4\pi\rho}{\beta} \sum_{\alpha i} \int drr^2 \left[-c_{\alpha i}(r) - \frac{1}{2} h_{\alpha i}(r) c_{\alpha i}(r) + \frac{1}{2} \{h_{\alpha i}(r)\}^2 \Theta\{-h_{\alpha i}(r)\} \right] \quad (3)$$

where $\Theta(x)$ represents the Heaviside step function.^{2,33} Greek subscripts, α, γ, \dots , refer to the interaction sites of the solute, and Roman subscripts, i, j, \dots , denote those of the solvent molecules. h and c represent the total and direct correlation functions, respectively. $\beta = 1/k_B T$ is the inverse temperature, where k_B and T are the Boltzmann constant and absolute temperature, respectively. We refer to the SFE expressions in eqs 2 and 3 as 1D-HNC and 1D-KH, respectively. It is noted that $\Delta\mu^{\text{HNC}}$ and $\Delta\mu^{\text{KH}}$ contain unphysical terms, $\{h_{\alpha i}(r)\}^2$ in the integrand, the contribution of which increases monotonically with the number of auxiliary sites. In addition, the SFE expression under the assumption of Gaussian fluctuation (GF) of the solvent distribution, 1D-GF, is given as⁵⁵

$$\Delta\mu^{\text{GF}} = \frac{4\pi\rho}{\beta} \sum_{\alpha i} \int drr^2 \left\{ -c_{\alpha i}(r) - \frac{1}{2} h_{\alpha i}(r) c_{\alpha i}(r) \right\} \quad (4)$$

Considering the 3D generalization of the Singer–Chandler expression, the SFEs in 3D-RISM of HNC, KH, and GF are given by^{33,44,55–57}

$$\Delta\mu^{\text{HNC}} = \frac{\rho}{\beta} \sum_i \int d\mathbf{r} \left[-c_i(\mathbf{r}) - \frac{1}{2} h_i(\mathbf{r}) c_i(\mathbf{r}) + \frac{1}{2} \{h_i(\mathbf{r})\}^2 \right] \quad (5)$$

$$\Delta\mu^{\text{KH}} = \frac{\rho}{\beta} \sum_i \int d\mathbf{r} \left[-c_i(\mathbf{r}) - \frac{1}{2} h_i(\mathbf{r}) c_i(\mathbf{r}) + \frac{1}{2} \{h_i(\mathbf{r})\}^2 \Theta\{-h_i(\mathbf{r})\} \right] \quad (6)$$

$$\Delta\mu^{\text{GF}} = \frac{\rho}{\beta} \sum_i \int d\mathbf{r} \left\{ -c_i(\mathbf{r}) - \frac{1}{2} h_i(\mathbf{r}) c_i(\mathbf{r}) \right\} \quad (7)$$

These expressions, eq 5–7, are denoted as 3D-HNC, 3D-KH, and 3D-GF, respectively.

2.2. Repulsive Bridge Correction (RBC). RBC is a correction method that introduces the intramolecular

correlation function of the solvent as a bridge correction in the closure equation.⁴⁴ For 1D-RISM, the following bridge correction is added to the HNC closure

$$\exp\{b_{ai}(r)\} = \prod_{j \neq i}^n [\bar{\omega}_{ji}(r) * \exp\{-\beta u_{aj}^R(r)\}] \quad (8)$$

where $\bar{\omega}$ represents the intramolecular correlation function of the solvent; n , the number of solvent interaction sites; u^R , the short-range core repulsion function; and $*$, a convolution integral. In this study, we employed the repulsive term in the LJ potential, u^R . The SFE of the 1D-RISM/HNC+RBC closure is obtained using the thermodynamic perturbation theory (TPT), 1D-HNC+RBC, as

$$\Delta\mu^{\text{HNC+RBC-TPT}} = \Delta\mu^{\text{HNC}} + \frac{4\pi\rho}{\beta} \sum_{ai} \int dr r^2 [\{h_{ai}^{\text{HNC}}(r) + 1\} \{\exp\{b_{ai}(r)\} - 1\}] \quad (9)$$

where the correlation functions, $h_{ai}^{\text{HNC}}(r)$ and $\Delta\mu^{\text{HNC}}$, are obtained in the absence of the bridge correction.

For 3D-RISM, the bridge function of RBC has the following form

$$\exp\{b_i(\mathbf{r})\} = \prod_{j \neq i}^n [\bar{\omega}_{ji} * \exp\{-\beta u_j^R(\mathbf{r})\}] \quad (10)$$

We employed the repulsive term in the LJ potential as the short-range core repulsion function, u^R , as with the 1D-RISM theory. The SFE expression of 3D-RISM/HNC+RBC, referred to as 3D-HNC+RBC, is obtained by TPT, as in the 1D-RISM case:

$$\Delta\mu^{\text{HNC+RBC-TPT}} = \Delta\mu^{\text{HNC}} + \frac{\rho}{\beta} \sum_i \int d\mathbf{r} [\{h_i^{\text{HNC}}(\mathbf{r}) + 1\} \{\exp\{b_i(\mathbf{r})\} - 1\}] \quad (11)$$

where the correlation functions are taken for $b_i(\mathbf{r}) = 0$, and $\Delta\mu^{\text{HNC}}$ is obtained using eq 5.

The KH+RBC SFE expressions are obtained using the same bridge correction to the KH closure, i.e., the RDF with KH+RBC is

$$g_{ai}^{\text{KH+RBC}}(r) = \exp\{b_{ai}(r)\} g_{ai}^{\text{KH}}(r) \quad (12)$$

where g_{ai}^{KH} is the RDF of the KH closure. The spatial distribution function in 3D-RISM/KH+RBC is also given in a similar manner. Using the TPT, the SFE expressions become

$$\Delta\mu^{\text{KH+RBC-TPT}} = \Delta\mu^{\text{KH}} + \frac{4\pi\rho}{\beta} \sum_{ai} \int dr r^2 [\{h_{ai}^{\text{KH}}(r) + 1\} \{\exp\{b_{ai}(r)\} - 1\}] \quad (13)$$

for 1D-RISM, and

$$\Delta\mu^{\text{KH+RBC-TPT}} = \Delta\mu^{\text{KH}} + \frac{\rho}{\beta} \sum_i \int d\mathbf{r} [\{h_i^{\text{KH}}(\mathbf{r}) + 1\} \{\exp\{b_i(\mathbf{r})\} - 1\}] \quad (14)$$

for 3D-RISM. The correlation functions in eqs 13 and 14 are obtained for $b_{ai}(r) = 0$ and $b_i(\mathbf{r}) = 0$, respectively. The SFEs by eqs 13 and 14 are denoted as 1D-KH+RBC and 3D-KH+RBC, respectively. Details of the derivation of 1D-KH+RBC and 3D-KH+RBC can be found in the Supporting Information (SI).

2.3. Distributed Partial Wave (PW) Expansion. The SFE expression of the PW expansion in 1D-RISM correlation functions, referred to as 1D-PW, has the following form:⁴⁰

$$\Delta\mu^{\text{PW}} = \frac{4\pi\rho}{\beta} \sum_{ai} \int dr r^2 \left\{ -c_{ai}(r) - \frac{1}{2} h_{ai}(r) c_{ai}(r) + \frac{1}{2} h_{ai}(r) h_{ai}^{\text{PW}}(r) \right\} \quad (15)$$

where

$$h_{ai}(\mathbf{r}_\alpha - \mathbf{r}_i) = \sum_{rj} \omega_{aj} * h_{rj}^{\text{PW}} * \bar{\omega}_{ji}(\mathbf{r}_\alpha - \mathbf{r}_i) \quad (16)$$

and where ω represents the intramolecular correlation function of the solute molecule; \mathbf{r}_α and \mathbf{r}_i , the relative positions of solute site α and solvent site i , respectively; and $h^{\text{PW}}(r)$, the PW component of the total correlation function.

We derive the 3D-RISM SFE variant of PW, 3D-PW, as

$$\Delta\mu^{\text{PW}} = \frac{\rho}{\beta} \sum_i \int d\mathbf{r} \left\{ -c_i(\mathbf{r}) - \frac{1}{2} h_i(\mathbf{r}) c_i(\mathbf{r}) + \frac{1}{2} h_i(\mathbf{r}) h_i^{\text{PW}}(\mathbf{r}) \right\} \quad (17)$$

where

$$h_i(\mathbf{r}) = \sum_j h_j^{\text{PW}} * \bar{\omega}_{ji}(\mathbf{r}) \quad (18)$$

The detail of the derivation of the SFE by the 3D-RISM theory based on PW is provided in the SI.

3. COMPUTATIONAL DETAILS

We use 467 small organic molecules taken from the test set of Rizzo et al.,⁵⁸ subsequently augmented by Mobley et al.⁵³ with extensive FEP results (see Table S1 in the SI). It is noted that the former study employed 504 molecules. However, our RISM-HNC calculations did not converge for some of these molecules, so they were excluded from the analysis. The geometries of the solute molecules are optimized at Hartree–Fock/6-31G(d) *in vacuo*. The LJ parameters for the solute molecules are obtained from the general Amber force field (GAFF) parameter set assigned by Antechamber.⁵⁹ The extended simple point charge (SPC/E) model⁶⁰ is used for the solvent water with modified hydrogen parameters ($\sigma_{\text{H}} = 1.0 \text{ \AA}$ and $\varepsilon_{\text{H}} = 0.046 \text{ kcal mol}^{-1}$). The LJ parameters of the hydroxy and protic hydrogens of solute molecules (alcohols, phenols, and acetic acid) are set to $\sigma_{\text{H}} = 1.0 \text{ \AA}$ and $\varepsilon_{\text{H}} = 0.046 \text{ kcal mol}^{-1}$ for the 1D-RISM adaptation. The Lorentz–Berthelot combination rule is applied in the calculations of the LJ parameters between different sites. The restraint electrostatic potential (RESP) method has been used to

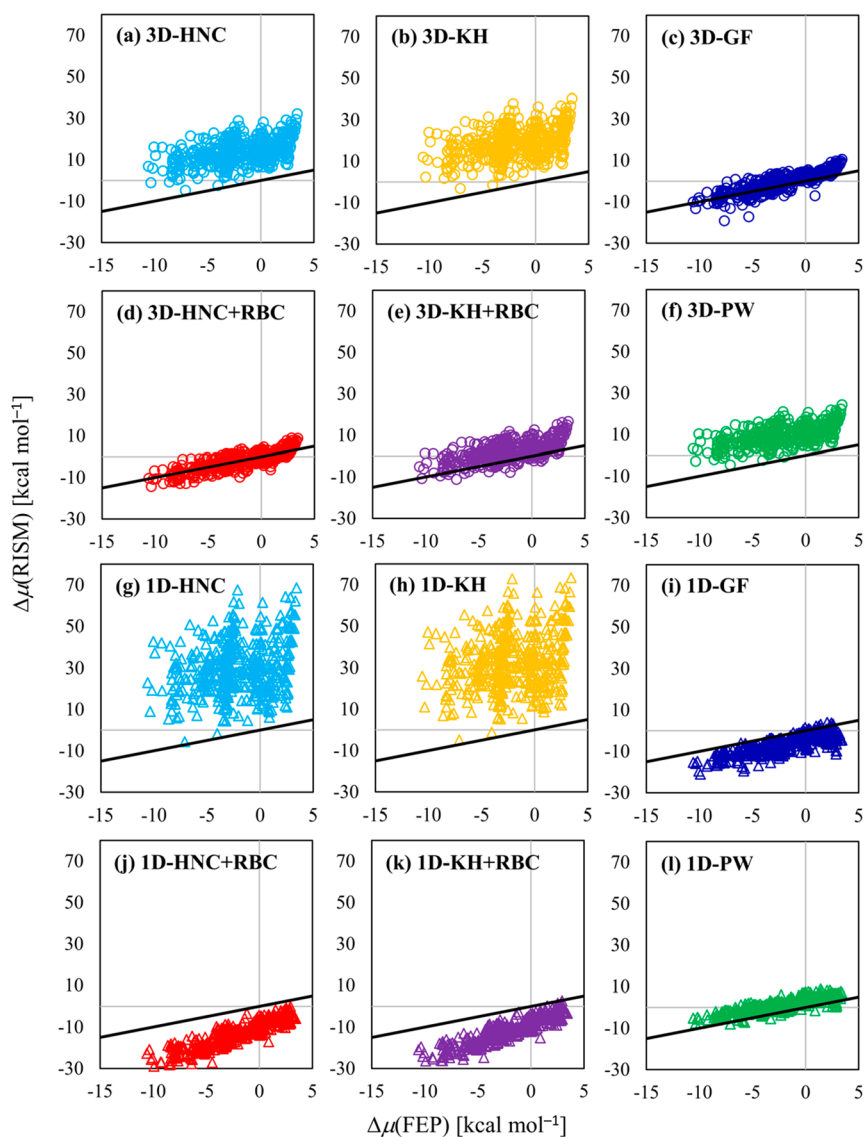


Figure 1. Comparison of the RISM SFEs with the FEP results. The solid black line represents $y = x$; open circles are results of 3D-RISM calculations; open triangles are results of 1D-RISM calculations.

determine the atomic partial charges on the solute sites.⁶¹ The number density of the solvent water and temperature are $0.03334 \text{ molecules } \text{Å}^{-3}$ and 298.0 K , respectively. The number of grid points is 2048 with a grid spacing of 0.05 Å for the 1D-RISM calculations. For the 3D-RISM calculations, the grid is 256^3 with a spacing of 0.25 Å . The modified direct inversion in the iterative subspace (MDIIS)⁶² is used to converge the 1D- and 3D-RISM equations, where the convergence threshold is 10^{-8} with respect to the root-mean-square deviation (RMSD) of the correlation functions. The correlation functions of 1D-RISM/HNC or 3D-RISM/HNC are used for the GF, RBC-TPT, and PW SFE expressions.

The above force field parameters for the solute and solvent molecules differ from those of Mobley et al.⁵³ Furthermore, we performed SFE calculations with the same force field parameters used by Mobley et al., and no significant difference was found in the results. (The results for Mobley's force field are summarized in Figure S2 and Table S3 in the Supporting Information.) In the present study, Mobley's parameter sets only converged for 450 molecules; therefore, we employed the GAFF parameter set for further analysis.

The geometrical optimization, LJ parametrization, and RESP calculations of the solute were performed using the Gaussian 09 Revision E.01 package.⁶³ All 1D- and 3D-RISM calculations were performed with an in-house RISM/3D-RISM code.⁶⁴

4. RESULTS AND DISCUSSION

4.1. SFE Component Analysis. The SFE of 1D- and 3D-RISM with various SFE expressions are compared with the FEP result by Mobley et al.,⁵³ as shown in Figure 1. The vertical and horizontal axes represent the SFEs of RISM and FEP, respectively. Normal distribution functions of the SFE error are plotted in Figure 2, and the root-mean-squared error (RMSE) from the FEP results and the coefficients of determination (R^2) from the linear regression fit are shown in Table 1.

At first glance, the *uncorrected* HNC and KH closures show a serious discrepancy from FEP with broad normal distributions. (The maximum errors are about 75 and 40 kcal mol^{-1} for 1D and 3D, respectively.) It can be seen that both RBC and PW afford relatively accurate SFEs in both the 1D- and 3D-RISM cases. Moreover, the normal distributions are significantly

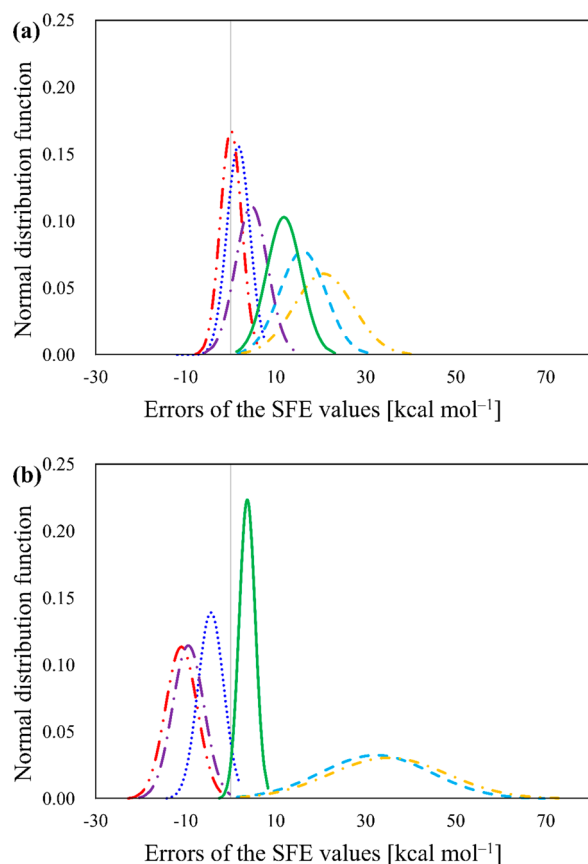


Figure 2. Normal distribution functions of SFE errors by (a) 3D-RISM and (b) 1D-RISM. Color code: light blue dashed lines, HNC; yellow dash-dotted lines, KH; blue dotted lines, GF; red long dash-two-dotted lines, HNC+RBC; purple long dash-dotted lines, KH+RBC; and green solid lines, PW.

Table 1. RMSEs of RISM SFE from FEP and Coefficients of Determination (R^2) and Their Electrostatic and Nonpolar Components^a

| SFE expression | RMSE (R^2) | | |
|----------------|----------------|---------------|---------------|
| | Total | Nonpolar | Electrostatic |
| 3D-HNC | 16.80 (0.232) | 17.34 (0.133) | 1.25 (0.856) |
| 3D-KH | 21.66 (0.139) | 22.10 (0.109) | 1.19 (0.852) |
| 3D-GF | 3.07 (0.738) | 3.80 (0.450) | 2.68 (0.782) |
| 3D-HNC+RBC | 2.38 (0.671) | 2.00 (0.423) | 1.40 (0.853) |
| 3D-KH+RBC | 5.86 (0.433) | 6.16 (0.243) | 1.28 (0.849) |
| 3D-PW | 12.45 (0.311) | 12.32 (0.179) | 1.02 (0.851) |
| 1D-HNC | 34.52 (0.056) | 36.41 (0.098) | 2.43 (0.869) |
| 1D-KH | 37.41 (0.049) | 39.35 (0.094) | 2.47 (0.869) |
| 1D-GF | 5.24 (0.613) | 3.62 (0.004) | 2.34 (0.858) |
| 1D-HNC+RBC | 11.49 (0.789) | 8.51 (0.283) | 3.30 (0.829) |
| 1D-KH+RBC | 10.04 (0.797) | 7.05 (0.330) | 3.30 (0.826) |
| 1D-PW | 4.09 (0.705) | 4.47 (0.031) | 1.22 (0.833) |

^aThe R^2 values are given in parentheses. The RMSEs are given in kcal mol⁻¹.

improved by RBC and PW application. These results clearly show that the introduction of the orientational correlation improves the SFE. The SFE expressions in 3D-RISM provide a more accurate SFE than those in the 1D-RISM theory, except for those based on PW. 3D-GF, 3D-HNC+RBC, and 3D-KH+RBC provide SFEs nearly consistent with or slightly higher

than the FEP results. In particular, 3D-HNC+RBC is the most accurate among the SFE expressions used in this study (RMSE = 2.38 kcal mol⁻¹). 1D-GF, 1D-HNC+RBC, and 1D-KH+RBC provide SFEs that are significantly underestimated by 15–20 kcal mol⁻¹. Although these corrections improve HNC and KH, the result appears to be overcorrected. In contrast to that of RBC, 1D-PW exhibits better RMSE and a normal distribution compared to that of 3D-PW.

To clarify the origin of the errors, we evaluate the nonpolar, $\Delta\mu_{np}$, and the electrostatic, $\Delta\mu_{ele}$, components of the SFE. These components are computed individually in two steps: $\Delta\mu_{np}$ is obtained by setting the solute partial charges to zero and subtracting $\Delta\mu_{np}$ from $\Delta\mu$ for $\Delta\mu_{ele}$, i.e., $\Delta\mu_{ele} = \Delta\mu - \Delta\mu_{np}$.¹⁹ These components are compared with those of FEP⁵³ in Figures 3 and 4. The RMSE and coefficients of determination are summarized in Table 1.

First, we consider the nonpolar components, $\Delta\mu_{np}$, in Figure 3. The uncorrected HNC and KH results are significantly deviated from FEP. The RMSEs of $\Delta\mu_{np}$ are in an order comparable to those of the total SFE for each SFE, indicating that the main source of the error of RISM SFE is the imprecise estimation of $\Delta\mu_{np}$ as indicated by Truchon et al.¹⁹ GF generally outperforms HNC and KH, although 1D-GF provides slightly underestimated results.

Both RBC and PW significantly improve the accuracy of $\Delta\mu_{np}$, and 3D-HNC+RBC is the most accurate in this study. Notably, the behaviors of RBC and PW differ remarkably between the 1D- and 3D-RISM cases. In what follows, we closely discuss RBC and PW separately.

By introducing RBC, the $\Delta\mu_{np}$ of 1D-HNC decreases drastically by 8–81 kcal mol⁻¹ and becomes lower than that of FEP. For 3D-HNC+RBC, the $\Delta\mu_{np}$ also decreases; however, the magnitude of the correction is smaller than that in the 1D case (range of correction is 6–26 kcal mol⁻¹). Consequently, 3D-HNC+RBC shows good agreement with the FEP results. The results of KH+RBC show a similar tendency with those of HNC+RBC. For both 1D and 3D, the magnitudes of correction by KH+RBC are almost the same as those by HNC+RBC (i.e., 8–83 and 6–26 kcal mol⁻¹ for 1D and 3D, respectively). As KH exhibits higher values than HNC (see Figure 3(a, b, g, and h)), 1D-KH+RBC and 3D-KH+RBC exhibit higher values than 1D-HNC+RBC and 3D-HNC+RBC, respectively. Although 3D-KH+RBC slightly underperforms 3D-HNC+RBC, the SFE of 3D-KH was significantly improved by introducing RBC. These results indicate that 3D-KH+RBC can provide the SFE with relatively good accuracy while retaining the feature of stable numerical convergence of the KH closure.

Introducing the PW also decreases $\Delta\mu_{np}$, although the magnitude of the correction is slightly smaller than that of RBC (the correction ranges in 3–67 kcal mol⁻¹ for 1D and 1–9 kcal mol⁻¹ for 3D). In particular, 1D-PW exhibits excellent consistency with the FEP results. These results highlight the interesting feature of the PW expansion. The PW expansion may effectively provide not only the correction for the errors caused by ISM, but also the correction for the lack of the bridge function because the RISM-SFE errors originate from both of them. Conversely, relatively large errors remain in 3D-PW. Since the PW expansion is applied to solvent only in 3D-RISM, the errors due to the lack of the bridge function are not correctable as in 1D-PW.

Next, we consider the results of the electrostatic components of the SFEs, $\Delta\mu_{ele}$. In Figure 4, $\Delta\mu_{ele}$ exhibits good correlation

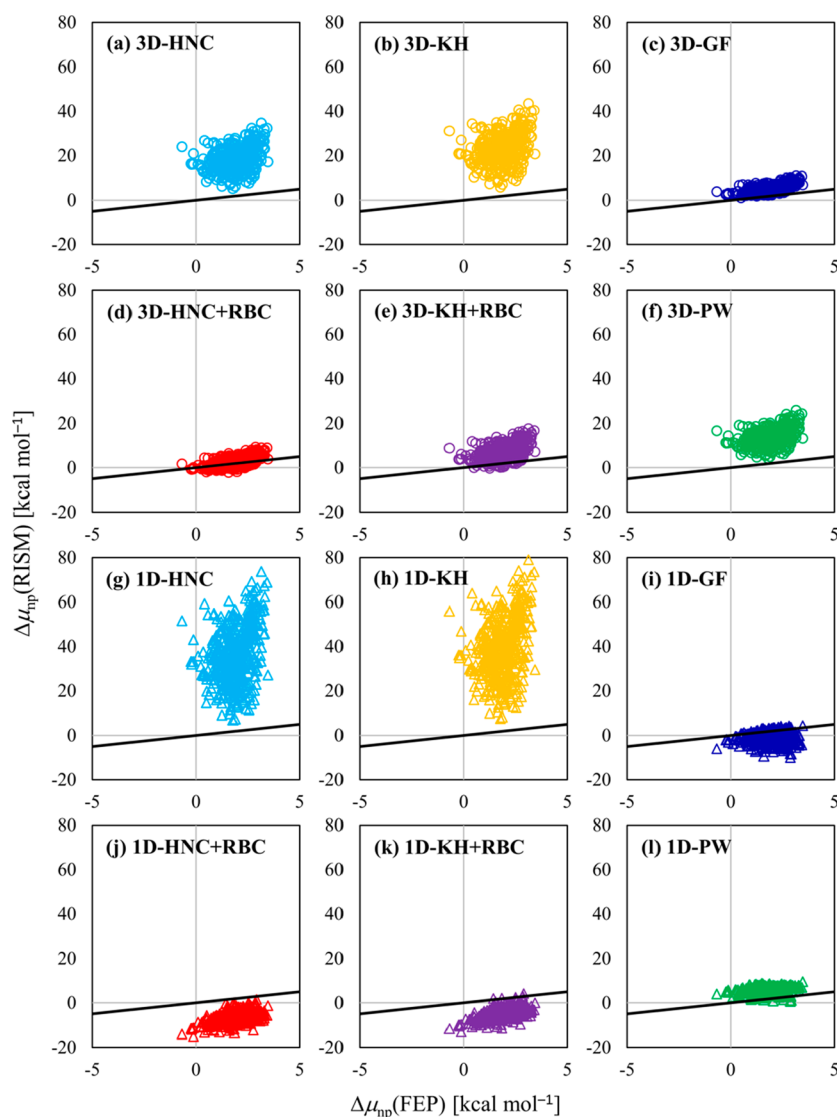


Figure 3. Comparison of the nonpolar components of RISM SFEs with the FEP results. The solid black line represents $y = x$; open circles are results of 3D-RISM; open triangles are results of 1D-RISM. (See also Figure S1 for close up views of panels (c), (d), (e), (f), (i), (j), (k), and (l)).

with the FEP results, and the errors are small compared with the case of $\Delta\mu_{\text{np}}$ (RMSEs are 1–4 kcal mol⁻¹). These results are in good agreement with those reported by Truchon et al. for 3D-KH.¹⁹ In particular, the accuracy of the 3D-RISM SFEs, except for 3D-GF, is overall preferable. This is because 3D-RISM considers the anisotropy of the solute molecule. 1D-RISM SFEs are slightly underestimated with some discrepancy, although 1D-PW exhibits good accuracy. The accuracy of $\Delta\mu_{\text{ele}}$ was deteriorated by applying RBC to both 1D- and 3D-RISM. As reported previously,⁴⁴ RBC is suitable for correcting the hydrophobic repulsive interaction between solute and solvent molecules but not for electrostatic interactions. In contrast, 1D-PW and 3D-PW improve the accuracy of $\Delta\mu_{\text{ele}}$ and 3D-PW is the most accurate among the SFE expressions in this study.

4.2. Assessment of Solute Site-Number Dependence of SFE Errors. In the RISM framework, the errors in SFE are known to increase monotonically with the number of solute sites.^{40,41,46} Since these errors disappear in the extended atom limit, the accuracy of SFE is considered to be crucial for the description of chemical reactions and molecular assemblies. To

elucidate the site-number dependency of the SFE errors, we evaluated the correlation between the number of solute sites and the deviations of RISM SFE from the FEP results.⁵³ In Figure 5, the differences between the RISM SFE and the FEP, $\Delta\Delta\mu = \Delta\mu_{\text{RISM}} - \Delta\mu_{\text{FEP}}$, are plotted against the number of solute sites. The results of the linear fitting are also superimposed in the figure.

For HNC and KH, $\Delta\Delta\mu$ increases monotonically with the number of solute sites, as reported in the literatures,^{40,41,46,48,49} and the degrees of the increase are somewhat reduced for 3D-HNC and 3D-KH (gradients are 0.79 and 1.03, respectively) compared with those for 1D-HNC and 1D-KH (gradients are 1.99 and 2.11, respectively). (It is noted that units for the gradients in Figure 5 are given by kcal mol⁻¹ (number of sites)⁻¹.) Therefore, the incorporation of the orientational correlation by 3D treatment certainly contributes to the correction of the site-number dependence of the SFE errors. Furthermore, 1D-GF and 3D-GF exhibit a relatively weak dependence. That is, the $\Delta\Delta\mu$ values for 1D-GF monotonically increase negatively with the number of solute sites, and

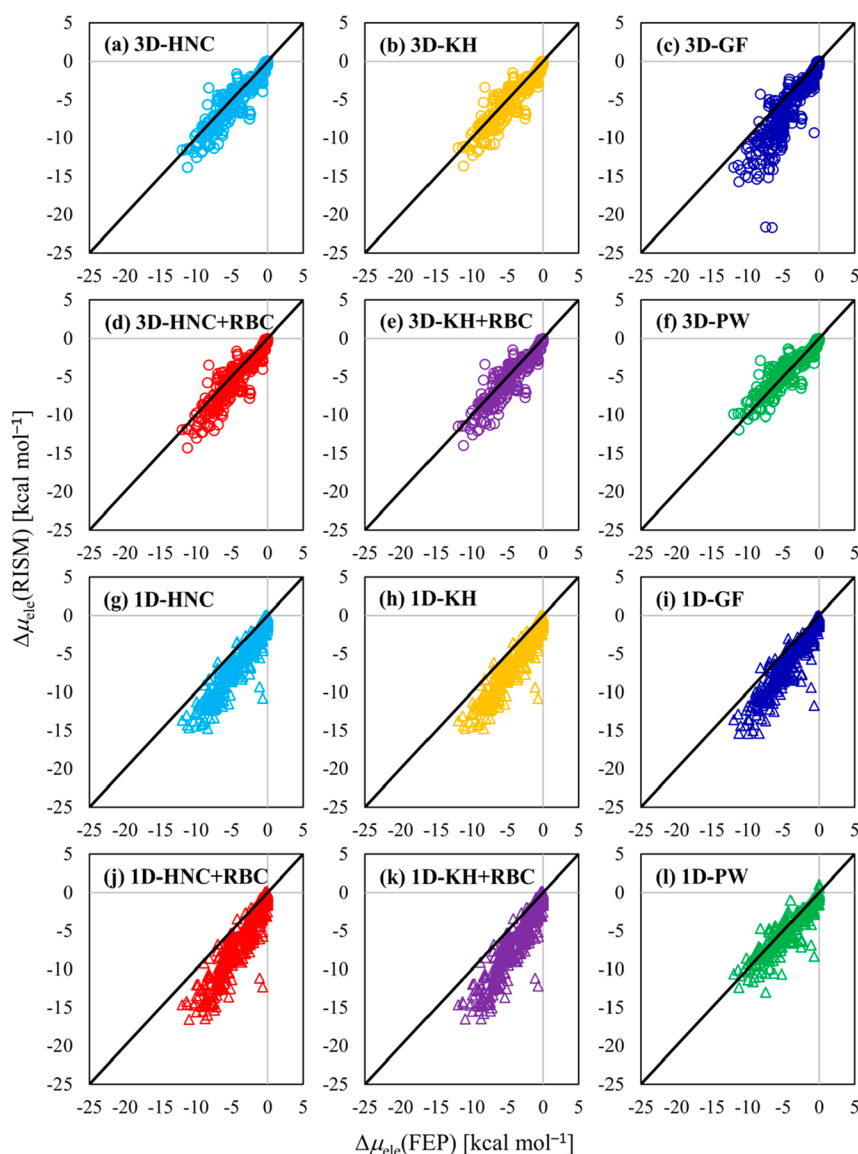


Figure 4. Comparison of the electrostatic components of RISM SFEs with FEP results. The solid black line represents $y = x$; open circles are results of 3D-RISM; open triangles are results of 1D-RISM.

those for 3D-GF increase positively (gradients are -0.37 and 0.21 , respectively).

By introducing the RBC and PW, the degree of solute site-number dependence significantly decreased. The trend of the solute site-number dependence is clearly different between in 1D- and 3D-RISM. 1D-PW has almost no solute site-number dependence of the SFE (gradient is only -0.06). Both 1D-HNC+RBC and 1D-KH+RBC have weak dependencies (gradients are -0.21 , and -0.15 , respectively). However, 3D-HNC+RBC, 3D-KH+RBC, and 3D-PW clearly exhibit solute site-number dependencies (gradients are 0.31 , 0.55 , and 0.60 , respectively), although these SFE expressions can somewhat suppress the degree of increase in $\Delta\Delta\mu$ compared with 3D-HNC and 3D-KH.

As described in Section 4.1, RBC and the PW expansion only introduce the orientational correlation of solvent part in 3D-RISM. Therefore, the defects in the solute part in 3D-RISM affect the solute site-number dependence of $\Delta\Delta\mu$ in 3D-HNC+RBC, 3D-KH+RBC, and 3D-PW, unlike in the 1D cases.

4.3. Relationship to Bulk Solvent Pressure with SFE.

The pressure correction (PC) method is one of the most successful correction methods for 3D-RISM SFE. It is suggested that the bulk solvent pressure based on 3D-RISM is dramatically overestimated, and the $P\Delta V$ term is well correlated with the SFE error,²³ where P and ΔV mean the bulk solvent pressure and PMV of solute molecule, respectively. In this subsection, we consider the relationship between the bulk solvent pressure and SFE. The bulk solvent pressure can be defined by the work (free energy change) required to exclude the solvent from the macroscopic volume, starting from a uniform density solvent. This work can be evaluated by the SFE of solute molecules with a large repulsive core. In the same manner as Sergiievskiy et al.,²³ the bulk solvent pressures for the corresponding SFE expression are given as

$$P_{3D-GF} = P_{1D-GF} = \frac{\rho}{2\beta} - \frac{\rho^2}{2\beta} \sum_{ij} \hat{c}_{ij}^{\text{HNC}}(k=0) \quad (19)$$

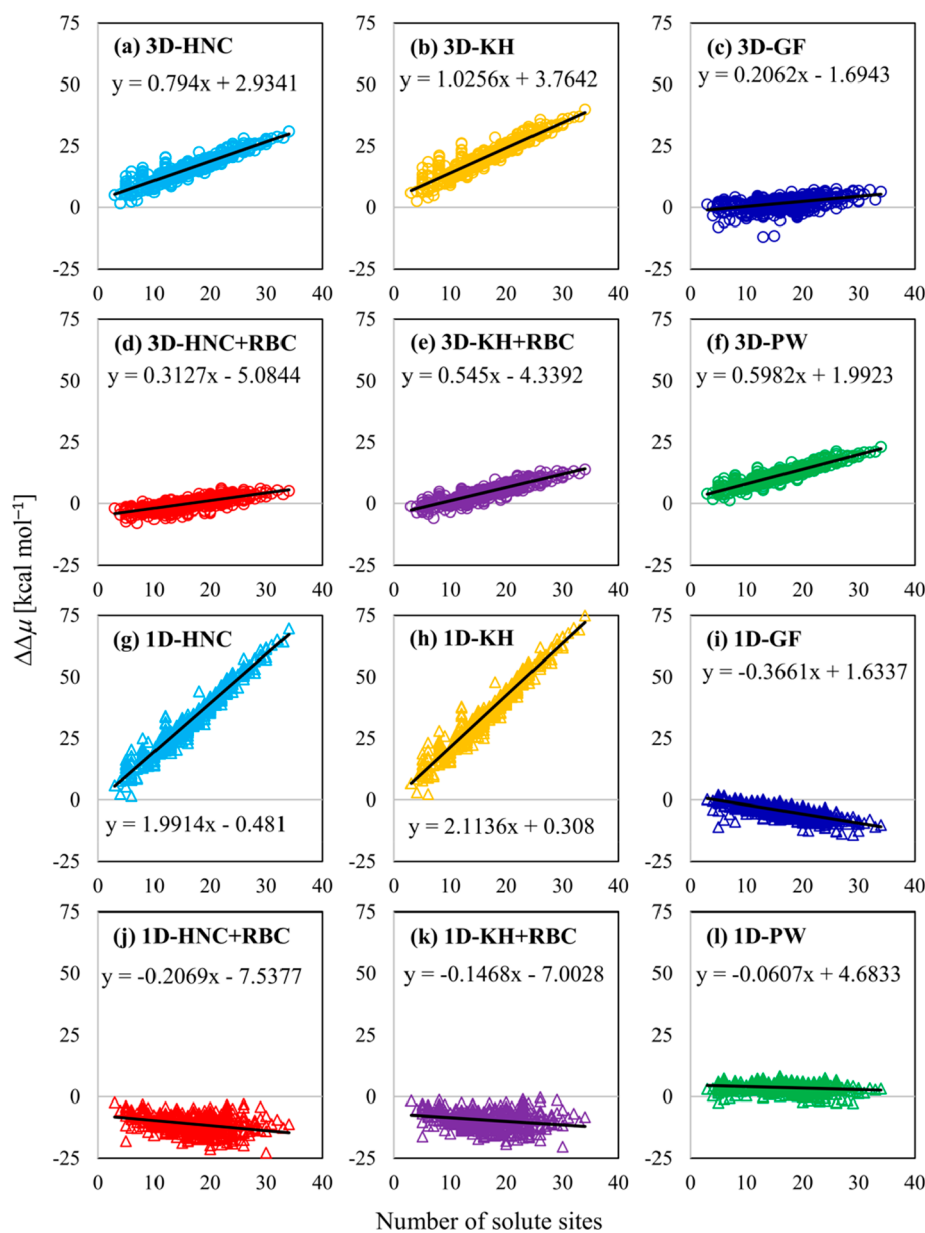


Figure 5. Correlation plots of the differences between the RISM SFEs and the FEP values, $\Delta\Delta\mu$, and the number of solute sites. The solid black line in each figure represents the linear regression fit; open circles are results of 3D-RISM; open triangles are results of 1D-RISM.

$$P_{3D-HNC} = P_{3D-RBC} = \frac{\rho}{2\beta}(n_s + 1) - \frac{\rho^2}{2\beta} \sum_{ij} \hat{c}_{ij}^{HNC}(k=0) \quad P_{3D-KH} = \frac{\rho}{2\beta}(n_s + 1) - \frac{\rho^2}{2\beta} \sum_{ij} \hat{c}_{ij}^{KH}(k=0) \quad (23)$$

$$= \frac{\rho}{2\beta}n_s + P_{3D-GF} \quad (20) \quad P_{1D-KH} = \frac{\rho}{2\beta}(n_u n_s + 1) - \frac{\rho^2}{2\beta} \sum_{ij} \hat{c}_{ij}^{KH}(k=0) \quad (24)$$

$$P_{1D-HNC} = P_{1D-RBC} = \frac{\rho}{2\beta}(n_u n_s + 1) - \frac{\rho^2}{2\beta} \sum_{ij} \hat{c}_{ij}^{HNC}(k=0) = \frac{\rho}{2\beta}n_u n_s + P_{3D-GF} \quad (21)$$

$$P_{3D-PW} = P_{1D-PW} = \frac{\rho}{\beta} - \frac{\rho^2}{2\beta} \sum_{ij} \hat{c}_{ij}^{HNC}(k=0) = \frac{\rho}{2\beta} + P_{3D-GF} \quad (22)$$

where \hat{c}_{ij}^{HNC} and \hat{c}_{ij}^{KH} are the solvent–solvent direct correlation functions in Fourier space obtained by RISM/HNC and RISM/KH, respectively. n_u and n_s denote the numbers of solute and solvent sites, respectively. The details of the derivation of these expressions are given in Section S2 of the Supporting Information. The 3D-HNC and 3D-RBC have the same pressure expression, which has a dependence on solvent site number, whereas the pressures for 1D-HNC and 1D-RBC depend on both solute and solvent site numbers. The GF and PW pressures have no site-number dependences, and they have the same formulas in 1D and 3D cases. These site-number

dependences correspond to those of the SFE.^{40,41,48,49} This means that the pressures determined by HNC, KH, and RBC-TPT show unphysical behavior for the addition of “auxiliary” sites. Therefore, the introduction of the orientational correlation by the PW expansion improves the pressure expression, whereas the RBC-TPT maintains the site-number dependence.

Based on eqs 19–24, the pressure must be

$$P_{1D-HNC} = P_{1D-RBC} \geq P_{3D-HNC} = P_{3D-RBC} \geq P_{3D-PW} = P_{1D-PW} > P_{3D-GF} = P_{1D-GF} \quad (25)$$

where the equality between 1D-HNC/RBC and 3D-HNC/RBC holds when $n_u = 1$ and that between 3D-HNC/RBC and 3D/1D-PW holds when $n_s = 1$. Similar trends to eq 25 can be found for the SFE error in Figure 1 and Table 1, except for the 1D/3D-RBC. The RBC-TPT does not affect the pressure expression; therefore, it achieves an improvement in the SFE regardless of pressure. In Table S7, the bulk solvent pressures evaluated by eqs 19–24 are summarized. It is worth noting that the pressure expressions with unphysical site-number dependence give significantly overestimated values.

From these pressure expressions, the PC terms can be readily evaluated. The PC term is given by

$$\Delta\mu_{PC} = -P\Delta V \quad (26)$$

where ΔV is the PMV.^{65–67} Note that the PMVs of RBC and PW are identical to that of HNC, as the PMV is determined solely by the solute–solvent correlation functions. The computed SFEs with the PC are compared with the FEP in Figure 6 and Figure S6, and the RMSEs of SFEs with the PC are summarized in Table 2. As reported by Sergiievskiy et al.,²³ the SFEs by 3D-HNC and 3D-KH are drastically improved by adding the PC. However, for most other cases, the SFEs are worsened by adding the PC except 3D-PW. In particular, the SFEs of RBC with the PC show larger deviations than those without the PC. Since the RBC does not affect pressure, the PC terms of 1D-HNC/RBC and 3D-HNC/RBC are identical to those of 1D-HNC and 3D-HNC, respectively. As a result of this fact, the PC terms are too large for the RBC SFEs. On the other hand, the 3D-PW with the PC shows relatively good performance as 3D-HNC with PC and 3D-KH with PC. This may be because the PC terms corrected the error due to the excluded volume of the solute that was not corrected by 3D-PW.

5. CONCLUSIONS

We have examined the effect of the solute–solvent orientational correlation on SFE of 1D- and 3D-RISM. Therefore, we used the RBC and PW expansion methods in conjunction with the KH and HNC closures to examine 1D-HNC, 1D-KH, 1D-GF, 1D-HNC+RBC, 1D-KH+RBC, 1D-PW, 3D-HNC, 3D-KH, 3D-GF, 3D-HNC+RBC, 3D-KH+RBC, and 3D-PW schemes, where 3D-PW was newly implemented in the present study. We computed the SFEs of these schemes in aqueous solutions for a set of small organic molecules. The results were compared with the simulation results.

Apparently, RBC and PW provide accurate SFE, compared to those of HNC and KH closures without corrections. These results show that incorporating the molecular orientations significantly contributes to improving the accuracy of SFE. In addition, the SFE component analysis demonstrated that the correction of the nonpolar component mainly contributes to

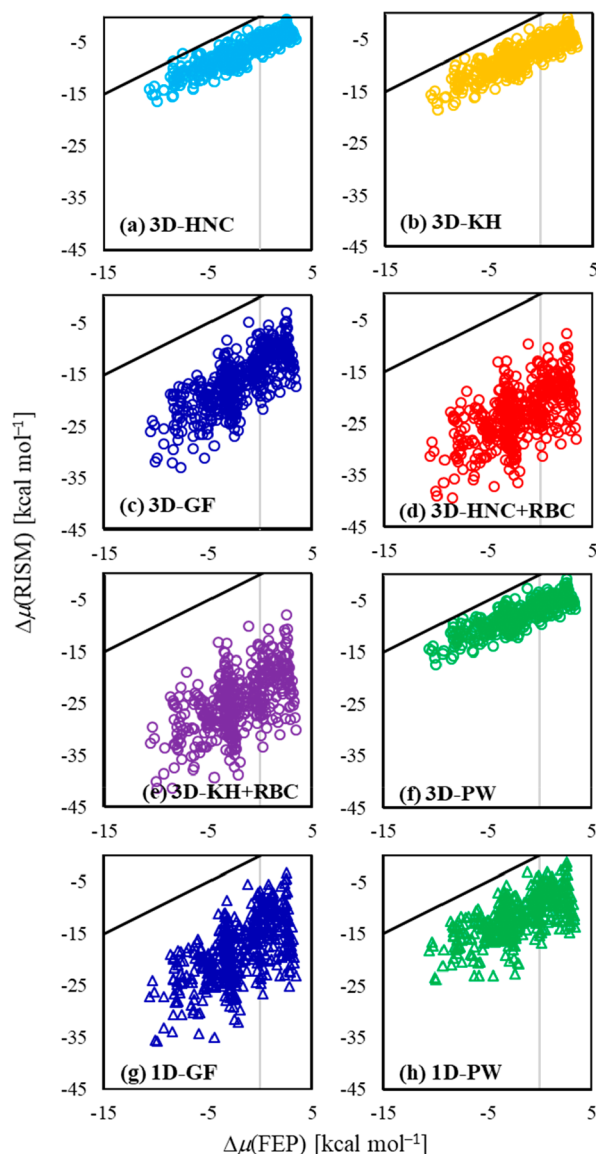


Figure 6. RISM SFEs with PC are compared with the FEP. The solid black line represents $y = x$; open circles are results of 3D-RISM calculations; open triangles are results of 1D-RISM calculations. Figures for 1D-HNC, 1D-HNC+RBC, 1D-KH, and 1D-KH+RBC are given in Figure S6.

the overall correction of the SFE values, indicating that the incorporation of the molecular orientations mainly affects the nonpolar component of SFE.

Conversely, it was found that the results of RBC and PW revealed different tendencies between 3D- and 1D-RISM. For 3D-RISM, RBC was more accurate than PW, while PW outperformed RBC for 1D-RISM. In addition, the error in SFE for 3D-HNC+RBC, 3D-KH+RBC, and 3D-PW increases as the number of solute sites increases, while no significant increase was found in the corresponding SFE expressions in 1D-RISM. Therefore, it appears that the corrections are insufficient in the 3D-RISM case, and a more sophisticated correction or closure equation is necessary.

The effects of the orientational correlation on the bulk solvent pressure and their relation to SFE have also been discussed. The PW expansion contributes to the improvement of the pressure expression, which removes unphysical behavior

Table 2. RMSEs of Pressure Corrected RISM SFE from FEP and Coefficients of Determination (R^2)^a

| SFE expression | RMSE | R^2 | Δ RMSE |
|----------------|-------|-------|---------------|
| 3D-HNC | 5.25 | 0.808 | -11.55 |
| 3D-KH | 6.51 | 0.754 | -15.15 |
| 3D-GF | 14.79 | 0.543 | 11.72 |
| 3D-HNC+RBC | 21.44 | 0.354 | 19.06 |
| 3D-KH+RBC | 22.80 | 0.327 | 16.94 |
| 3D-PW | 6.12 | 0.718 | -6.33 |
| 1D-HNC | 52.25 | 0.026 | 17.73 |
| 1D-KH | 49.43 | 0.028 | 12.02 |
| 1D-GF | 16.99 | 0.357 | 11.75 |
| 1D-HNC+RBC | 96.75 | 0.028 | 85.26 |
| 1D-KH+RBC | 95.25 | 0.029 | 85.21 |
| 1D-PW | 10.01 | 0.416 | 5.92 |

^aThe RMSEs are given in kcal mol⁻¹. Δ RMSE denotes the RMSE change from the RMSE without pressure correction.

related to the site-number dependence, whereas the RBC has no contribution to the pressure expression. In the present study, we have not discussed the PMV, which is one of the factors in the PC method. Because the same correlation function from the HNC is employed for the GF, RBC-TPT, and PW, there is no influence on the PMV from the viewpoint of the Kirkwood–Buff theory.^{65,66} However, if a closure equation corresponding to the PW is developed in the future, the influence of the orientational correlation on the PMV will also be considered.

All the cases examined in this study are for aqueous solutions. The previous studies have shown that 1D-PW is quantitatively accurate for the chloroform solution and the partition coefficient between water and chloroform.^{48,49} In contrast, the RBC for organic solvents behaves in a manner significantly different from that of an aqueous solution.⁴⁵ Therefore, further study on the orientational correlations for nonaqueous solutions is needed for more general insights.

■ ASSOCIATED CONTENT

■ Supporting Information

The Supporting Information is available free of charge on the ACS Publications website at DOI: 10.1021/acs.jcim.9b00330.

Derivation of KH+RBC and 3D-PW, derivation of pressure expressions, assessment of the conformational fluctuation of the solute molecule, and experimental and FEP SFE values of Mobley's test set. (PDF)

Structure and force field parameters for Mobley's test set. (TXT)

■ AUTHOR INFORMATION

Corresponding Author

*E-mail: noriwo@chem.kyushu-univ.jp.

ORCID

Shoichi Tanimoto: 0000-0001-6267-085X

Norio Yoshida: 0000-0002-2023-7254

Tsuyoshi Yamaguchi: 0000-0003-4590-8592

Haruyuki Nakano: 0000-0002-7008-0312

Funding

This work was supported by Grants-in-Aid (16H00842, 16K05519, 18K05036, and 19H02677) from the Ministry of Education, Culture, Sports, Science and Technology (MEXT), Japan. N.Y. also acknowledges support from the Toyota

RIKEN Scholar Program at the Toyota Physical and Chemical Research Institute. S.L.T. acknowledges the financial support of the MEXT as Priority Issue on Post-K computer (Development of new fundamental technologies for high-efficiency energy creation, conversion and/or storage, and use) and JSPS Grants-in-Aid for Scientific Research (A) (Grant No. JP18H03900).

Notes

The authors declare no competing financial interest.

■ ACKNOWLEDGMENTS

The authors are grateful to Prof. Ryo Akiyama (Kyushu University), Prof. Masahiro Higashi (Kyoto University), Prof. Tatsuhiko Miyata (Ehime University), and Prof. Yoshihiro Watanabe (Kyushu University) for helpful discussions.

■ REFERENCES

- (1) Chandler, D.; Andersen, H. C. Optimized Cluster Expansions for Classical Fluids. II. Theory of Molecular Liquids. *J. Chem. Phys.* **1972**, *57*, 1930–1937.
- (2) Hirata, F. *Molecular Theory of Solvation*; Springer Science & Business Media, 2003; Vol. 24.
- (3) Hirata, F.; Rossky, P. J. An Extended Rism Equation for Molecular Polar Fluids. *Chem. Phys. Lett.* **1981**, *83*, 329–334.
- (4) Beglov, D.; Roux, B. An Integral Equation To Describe the Solvation of Polar Molecules in Liquid Water. *J. Phys. Chem. B* **1997**, *101*, 7821–7826.
- (5) Kovalenko, A.; Hirata, F. Three-Dimensional Density Profiles of Water in Contact with a Solute of Arbitrary Shape: A RISM Approach. *Chem. Phys. Lett.* **1998**, *290*, 237–244.
- (6) Hong, J.; Yoshida, N.; Chong, S.-H.; Lee, C.; Ham, S.; Hirata, F. Elucidating the Molecular Origin of Hydrolysis Energy of Pyrophosphate in Water. *J. Chem. Theory Comput.* **2012**, *8*, 2239–2246.
- (7) Kasai, Y.; Yoshida, N.; Nakano, H. Theoretical Analysis of Salt Effect on Intramolecular Proton Transfer Reaction of Glycine in Aqueous NaCl Solution. *J. Mol. Liq.* **2014**, *200*, 32–37.
- (8) Kasai, Y.; Yoshida, N.; Nakano, H. Theoretical Analysis of Co-Solvent Effect on the Proton Transfer Reaction of Glycine in a Water-Acetonitrile Mixture. *J. Chem. Phys.* **2015**, *142*, 204103.
- (9) Hayaki, S.; Kido, K.; Yokogawa, D.; Sato, H.; Sakaki, S. A Theoretical Analysis of a Diels-Alder Reaction in Ionic Liquids. *J. Phys. Chem. B* **2009**, *113*, 8227–8230.
- (10) Yoshida, N.; Tanaka, H.; Hirata, F. Theoretical Study of Salt Effects on the Diels-Alder Reaction of Cyclopentadiene with Methyl Vinyl Ketone Using RISM-SCF Theory. *J. Phys. Chem. B* **2013**, *117*, 14115–14121.
- (11) Sato, H. A Modern Solvation Theory: Quantum Chemistry and Statistical Chemistry. *Phys. Chem. Chem. Phys.* **2013**, *15*, 7450–7465.
- (12) Yoshida, N.; Imai, T.; Phongphanphanee, S.; Kovalenko, A.; Hirata, F. Molecular Recognition in Biomolecules Studied by Statistical-Mechanical Integral-Equation Theory of Liquids. *J. Phys. Chem. B* **2009**, *113*, 873–886.
- (13) Yoshida, N. Role of Solvation in Drug Design as Revealed by the Statistical Mechanics Integral Equation Theory of Liquids. *J. Chem. Inf. Model.* **2017**, *57*, 2646–2656.
- (14) Tanimoto, S.; Higashi, M.; Yoshida, N.; Nakano, H. The Ion Dependence of Carbohydrate Binding of CBM36: An MD and 3D-RISM Study. *J. Phys.: Condens. Matter* **2016**, *28*, 344005.
- (15) Phongphanphanee, S.; Yoshida, N.; Oiki, S.; Hirata, F. Probing “Ambivalent” Snug-Fit Sites in the KcsA Potassium Channel Using Three-Dimensional Reference Interaction Site Model (3D-RISM) Theory. *Pure Appl. Chem.* **2014**, *86*, 97–104.
- (16) Chong, S.-H.; Ham, S. Impact of Chemical Heterogeneity on Protein Self-Assembly in Water. *Proc. Natl. Acad. Sci. U. S. A.* **2012**, *109*, 7636–7641.

- (17) Furukawa-Hagiya, T.; Yoshida, N.; Chiba, S.; Hayashi, T.; Furuta, T.; Sohma, Y.; Sakurai, M. Water-Mediated Forces between the Nucleotide Binding Domains Generate the Power Stroke in an ABC Transporter. *Chem. Phys. Lett.* **2014**, *616–617*, 165–170.
- (18) Palmer, D. S.; Frolov, A. I.; Ratkova, E. L.; Fedorov, M. V. Towards a Universal Method for Calculating Hydration Free Energies: A 3D Reference Interaction Site Model with Partial Molar Volume Correction. *J. Phys.: Condens. Matter* **2010**, *22*, 492101.
- (19) Truchon, J. F.; Pettitt, B. M.; Labute, P. A Cavity Corrected 3D-RISM Functional for Accurate Solvation Free Energies. *J. Chem. Theory Comput.* **2014**, *10*, 934–941.
- (20) Sumi, T.; Mitsutake, A.; Maruyama, Y. A Solvation-Free-Energy Functional: A Reference-Modified Density Functional Formulation. *J. Comput. Chem.* **2015**, *36*, 1359–1369.
- (21) Sumi, T.; Maruyama, Y.; Mitsutake, A.; Koga, K. A Reference-Modified Density Functional Theory: An Application to Solvation Free-Energy Calculations for a Lennard-Jones Solution. *J. Chem. Phys.* **2016**, *144*, 224104.
- (22) Sergiievskiy, V. P.; Jeanmairet, G.; Levesque, M.; Borgis, D. Fast Computation of Solvation Free Energies with Molecular Density Functional Theory: Thermodynamic-Ensemble Partial Molar Volume Corrections. *J. Phys. Chem. Lett.* **2014**, *5*, 1935–1942.
- (23) Sergiievskiy, V.; Jeanmairet, G.; Levesque, M.; Borgis, D. Solvation Free-Energy Pressure Corrections in the Three Dimensional Reference Interaction Site Model. *J. Chem. Phys.* **2015**, *143*, 184116.
- (24) Misin, M.; Palmer, D. S.; Fedorov, M. V. Predicting Solvation Free Energies Using Parameter-Free Solvent Models. *J. Phys. Chem. B* **2016**, *120*, 5724–5731.
- (25) Ratkova, E. L.; Palmer, D. S.; Fedorov, M. V. Solvation Thermodynamics of Organic Molecules by the Molecular Integral Equation Theory: Approaching Chemical Accuracy. *Chem. Rev.* **2015**, *115*, 6312–6356.
- (26) Misin, M.; Fedorov, M. V.; Palmer, D. S. Communication: Accurate Hydration Free Energies at a Wide Range of Temperatures from 3D-RISM. *J. Chem. Phys.* **2015**, *142*, 091105.
- (27) Misin, M.; Vainikka, P. A.; Fedorov, M. V.; Palmer, D. S. Salting-out Effects by Pressure-Corrected 3D-RISM. *J. Chem. Phys.* **2016**, *145*, 194501.
- (28) Roy, D.; Kovalenko, A. Performance of 3D-RISM-KH in Predicting Hydration Free Energy: Effect of Solute Parameters. *J. Phys. Chem. A* **2019**, *123*, 4087–4093.
- (29) Misin, M.; Fedorov, M. V.; Palmer, D. S. Hydration Free Energies of Molecular Ions from Theory and Simulation. *J. Phys. Chem. B* **2016**, *120*, 975–983.
- (30) Johnson, J.; Case, D. A.; Yamazaki, T.; Gusarov, S.; Kovalenko, A.; Luchko, T. Small Molecule Hydration Energy and Entropy from 3D-RISM. *J. Phys.: Condens. Matter* **2016**, *28*, 344002.
- (31) Luchko, T.; Blinov, N.; Limon, G. C.; Joyce, K. P.; Kovalenko, A. SAMPLS:3D-RISM Partition Coefficient Calculations with Partial Molar Volume Corrections and Solute Conformational Sampling. *J. Comput.-Aided Mol. Des.* **2016**, *30*, 1115–1127.
- (32) Sosnin, S.; Misin, M.; Palmer, D. S.; Fedorov, M. V. 3D Matters! 3D-RISM and 3D Convolutional Neural Network for Accurate Bioaccumulation Prediction. *J. Phys.: Condens. Matter* **2018**, *30*, 32LT03.
- (33) Kovalenko, A.; Hirata, F. Self-Consistent Description of a Metal-Water Interface by the Kohn-Sham Density Functional Theory and the Three-Dimensional Reference Interaction Site Model. *J. Chem. Phys.* **1999**, *110*, 10095–10112.
- (34) Chandler, D.; Silbey, R.; Ladanyi, B. M. New and Proper Integral Equations for Site-Site Equilibrium Correlations in Molecular Fluids. *Mol. Phys.* **1982**, *46*, 1335–1345.
- (35) Solana, J. R. *Perturbation Theories for the Thermodynamic Properties of Fluids and Solids*; CRC Press, 2013.
- (36) Miyata, T.; Thapa, J. Accuracy of Solvation Free Energy Calculated by Hypernetted Chain and Kovalenko-Hirata Approximations for Two-Component System of Lennard-Jones Liquid. *Chem. Phys. Lett.* **2014**, *604*, 122–126.
- (37) Miyata, T.; Miyazaki, S. Accuracy of Temperature-Derivative of Radial Distribution Function Calculated under Approximations in Ornstein-Zernike Theory for One-Component Lennard-Jones Fluid. *Chem. Phys. Lett.* **2016**, *658*, 224–229.
- (38) Miyata, T. A Parameterization of Empirical Sigma Enlarging Bridge Correction of Kovalenko-Hirata Closure in Ornstein-Zernike Theory for Lennard-Jones Fluids. *Bull. Chem. Soc. Jpn.* **2017**, *90*, 1095–1104.
- (39) Miyata, T.; Ebato, Y. Thermodynamic Significance to Correct the Location of First Rising Region in Radial Distribution Function Approximately Estimated from Ornstein-Zernike Integral Equation Theory for Lennard-Jones Fluids. *J. Mol. Liq.* **2016**, *217*, 75–82.
- (40) Ten-no, S. Free Energy of Solvation for the Reference Interaction Site Model: Critical Comparison of Expressions. *J. Chem. Phys.* **2001**, *115*, 3724–3731.
- (41) Ten-no, S.; Iwata, S. On the Connection between the Reference Interaction Site Model Integral Equation Theory and the Partial Wave Expansion of the Molecular Ornstein-Zernike Equation. *J. Chem. Phys.* **1999**, *111*, 4865–4868.
- (42) Furuhashi, A.; Ten-no, S. The Use of Distributed Partial Wave Basis for Accurate Atom-Molecule Statistical Distributions. *J. Chem. Phys.* **2002**, *117*, 4087–4094.
- (43) Furuhashi, A.; Ten-no, S. Integral Equation Theory of Distributed Partial Wave Basis: Application to Molecular Liquids. *Chem. Phys. Lett.* **2004**, *384*, 376–381.
- (44) Kovalenko, A.; Hirata, F. Hydration Free Energy of Hydrophobic Solutes Studied by a Reference Interaction Site Model with a Repulsive Bridge Correction and a Thermodynamic Perturbation Method. *J. Chem. Phys.* **2000**, *113*, 2793–2805.
- (45) Kido, K.; Yokogawa, D.; Sato, H. A Modified Repulsive Bridge Correction to Accurate Evaluation of Solvation Free Energy in Integral Equation Theory for Molecular Liquids. *J. Chem. Phys.* **2012**, *137*, 024106.
- (46) Yokogawa, D. Toward Accurate Solvation Free Energy Calculation with the Reference Interaction Site Model Self-Consistent Field: Introduction of a New Bridge Function. *J. Chem. Theory Comput.* **2018**, *14*, 3272–3278.
- (47) Chuev, G. N.; Fedorov, M. V.; Crain, J. Improved Estimates for Hydration Free Energy Obtained by the Reference Interaction Site Model. *Chem. Phys. Lett.* **2007**, *448*, 198–202.
- (48) Sato, K.; Chuman, H.; Ten-no, S. Comparative Study on Solvation Free Energy Expressions in Reference Interaction Site Model Integral Equation Theory. *J. Phys. Chem. B* **2005**, *109*, 17290–17295.
- (49) Ten-no, S.; Jung, J.; Chuman, H.; Kawashima, Y. Assessment of Free Energy Expressions in RISM Integral Equation Theory: Theoretical Prediction of Partition Coefficients Revisited. *Mol. Phys.* **2010**, *108*, 327–332.
- (50) Fujita, T.; Yamamoto, T. Assessing the Accuracy of Integral Equation Theories for Nano-Sized Hydrophobic Solutes in Water. *J. Chem. Phys.* **2017**, *147*, 014110.
- (51) Ebato, Y.; Miyata, T. A Pressure Consistent Bridge Correction of Kovalenko-Hirata Closure in Ornstein-Zernike Theory for Lennard-Jones Fluids by Apparently Adjusting Sigma Parameter. *AIP Adv.* **2016**, *6*, 055111.
- (52) Miyata, T.; Tange, K. Performance of Kobryn-Gusarov-Kovalenko Closure from a Thermodynamic Viewpoint for One-Component Lennard-Jones Fluids. *Chem. Phys. Lett.* **2018**, *700*, 88–95.
- (53) Mobley, D. L.; Bayly, C. I.; Cooper, M. D.; Shirts, M. R.; Dill, K. A. Small Molecule Hydration Free Energies in Explicit Solvent: An Extensive Test of Fixed-Charge Atomistic Simulations. *J. Chem. Theory Comput.* **2009**, *5*, 350–358.
- (54) Singer, S. J.; Chandler, D. Free Energy Functions in the Extended RISM Approximation. *Mol. Phys.* **1985**, *55*, 621–625.
- (55) Chandler, D.; Singh, Y.; Richardson, D. M. Excess Electrons in Simple Fluids. I. General Equilibrium Theory for Classical Hard Sphere Solvents. *J. Chem. Phys.* **1984**, *81*, 1975–1982.

(56) Kovalenko, A.; Hirata, F. Potentials of Mean Force of Simple Ions in Ambient Aqueous Solution. I. Three-Dimensional Reference Interaction Site Model Approach. *J. Chem. Phys.* **2000**, *112*, 10391–10402.

(57) Genheden, S.; Luchko, T.; Gusarov, S.; Kovalenko, A.; Ryde, U. An MM/3D-RISM Approach for Ligand Binding Affinities. *J. Phys. Chem. B* **2010**, *114*, 8505–8516.

(58) Rizzo, R. C.; Aynechi, T.; Case, D. A.; Kuntz, I. D. Estimation of Absolute Free Energies of Hydration Using Continuum Methods: Accuracy of Partial Charge Models and Optimization of Nonpolar Contributions. *J. Chem. Theory Comput.* **2006**, *2*, 128–139.

(59) Wang, J.; Wang, W.; Kollman, P. A.; Case, D. A. Automatic Atom Type and Bond Type Perception in Molecular Mechanical Calculations. *J. Mol. Graphics Modell.* **2006**, *25*, 247–260.

(60) Berendsen, H. J. C.; Grigera, J. R.; Straatsma, T. P. The Missing Term in Effective Pair Potentials. *J. Phys. Chem.* **1987**, *91*, 6269–6271.

(61) Bayly, C. I.; Cieplak, P.; Cornell, W. D.; Kollman, P. A. A Well-Behaved Electrostatic Potential Based Method Using Charge Restraints for Deriving Atomic Charges: The RESP Model. *J. Phys. Chem.* **1993**, *97*, 10269–10280.

(62) Kovalenko, A.; Ten-no, S.; Hirata, F. Solution of Three-Dimensional Reference Interaction Site Model and Hypernetted Chain Equations for Simple Point Charge Water by Modified Method of Direct Inversion in Iterative Subspace. *J. Comput. Chem.* **1999**, *20*, 928–936.

(63) Frisch, M. J.; Trucks, G. W.; Schlegel, H. B.; Scuseria, G. E.; Robb, M. A.; Cheeseman, J. R.; Scalmani, G.; Barone, V.; Mennucci, B.; Petersson, G. A.; Nakatsuji, H.; Caricato, M.; Li, X.; Hratchian, H. P.; Izmaylov, A. F.; Bloino, J.; Zheng, G.; Sonnenberg, J. L.; Hada, M.; Ehara, M.; Toyota, K.; Fukuda, R.; Hasegawa, J.; Ishida, M.; Nakajima, T.; Honda, Y.; Kitao, O.; Nakai, H.; Vreven, T.; Montgomery, J. A., Jr.; Peralta, J. E.; Ogliaro, F.; Bearpark, M.; Heyd, J. J.; Brothers, E.; Kudin, K. N.; Staroverov, V. N.; Kobayashi, R.; Normand, J.; Raghavachari, K.; Rendell, A.; Burant, J. C.; Iyengar, S. S.; Tomasi, J.; Cossi, M.; Rega, N.; Millam, J. M.; Klene, M.; Knox, J. E.; Cross, J. B.; Bakken, V.; Adamo, C.; Jaramillo, J.; Gomperts, R.; Stratmann, R. E.; Yazyev, O.; Austin, A. J.; Cammi, R.; Pomelli, C.; Ochterski, J. W.; Martin, R. L.; Morokuma, K.; Zakrzewski, V. G.; Voth, G. A.; Salvador, P.; Dannenberg, J. J.; Dapprich, S.; Daniels, A. D.; Farkas, Ö.; Foresman, J. B.; Ortiz, J. V.; Cioslowski, J.; Fox, D. J. *Gaussian 09*, revision E.01; Gaussian, Inc., Wallingford, CT, 2009.

(64) Yoshida, N.; Hirata, F. A New Method to Determine Electrostatic Potential around a Macromolecule in Solution from Molecular Wave Functions. *J. Comput. Chem.* **2006**, *27*, 453–462.

(65) Kirkwood, J. G.; Buff, F. P. The Statistical Mechanical Theory of Solutions. I. *J. Chem. Phys.* **1951**, *19*, 774–777.

(66) Imai, T.; Kovalenko, A.; Hirata, F. Partial Molar Volume of Proteins Studied by the Three-Dimensional Reference Interaction Site Model Theory. *J. Phys. Chem. B* **2005**, *109*, 6658–6665.

(67) Imai, T.; Kinoshita, M.; Hirata, F. Theoretical Study for Partial Molar Volume of Amino Acids in Aqueous Solution: Implication of Ideal Fluctuation Volume. *J. Chem. Phys.* **2000**, *112*, 9469–9478.